Al-Azhar University Civil Engineering Research Magazine (CERM)
Vol. (40) No. (3) July, 2018

EFFECT OF TIE BEAM DIMENSIONS ON FOOTINGS UNDER ECCENTRIC LOADING

Elsamny M.K[1] , Ezz-Eldeen H.A[2], Elbatal S.A[3] , Elsayed M.M[4]

1 Civil Engineering Department, Al-Azhar University, Cairo, Egypt
2 Civil Engineering Department, Al-Azhar University, Cairo, Egypt
3 Civil Engineering Department, Al-Azhar University, Cairo, Egypt
4 Faculty of engineering, Sinai University, North Sinai- ElArish-El Masaid, Egypt

ملخص:

تهدف هذه الدراسة لمعرفة مدى تأثير القواعد المحملة بحمل مركزى على الهبوط وقيم العزوم والقص وأيضا الازاحه الأفقية وقد تم دراسة تأثير كلا من سمك وعرض الشداد وكذلك نوع تربة التأسيس على الهبوط والازاحه الافقية فى الاتجاهين XوZ وكذلك قيم ضغط التلامس اسفل الأساسات. و تم إستخدام نموذج ثلاثى الأبعاد مكون من 16 قاعدة وكانت ابعاد هذه القواعد كالأتى(قواعد الركن (2.0*2.0)م والقواعد الطرفية (2.50*2.50)م والقواعد الوسطى (3.0*3.0)م بينما فى حالة وجود الجار تختلف أبعاد هذه القواعد وتصبح كالأتى (قواعد الركن (1.0*1.0)م والقواعد الطرفية (1.0*2.0)م والقواعد الوسطى (1.50*2.50)م) .وسمك هذه القواعد ثابت = 0.5م وكل هذه القواعد مربوطة بشدادات وعند مناسيب مختلفة . وتم دراسة هذة المتغيرات على الهبوط وضغط التلامس والعزوم لهذه القواعد. و تم عمل هذا النموذج باستخدام برنامج العناصر المحددة (finite element) لدراسة الهبوط وضغط التلامس لهذه القواعد .وقد اظهرت النتائج المكتسبة من هذا البحث أن قيم الهبوط والازاحة الأفيقة فى الإتجاهين(X, Z) تقل كلما زاد عرض وإرتفاع الميدة وذلك بنسبة تتراوح من (20 الى 40)%. وايضا قيم ضغط التلامس تقل بزيادة إرتفاع وعرض الشداد بنسبة تتراوح من (30 الى 40)%. كما وجد ان قيم العزوم وقوى القص تقل كما زادت أبعاد الشداد وذلك بنسبة تتراوح من (30 الى 40)%.

ABSTRACT

The aim of this study is to investigate the effect of thickness and width of tie beams on footings under eccentric loading. The chosen model contains 16 footings connected with tie beams. However the effect of thickness and width of tie beams on vertical and horizontal displacement as well as the contact pressure, moment and shear have been investigated. The footing dimensions are (2.0*2.0) m for corner footings, (2.50*2.50) m for edge footings and (3.0*3.0) m for middle footings). The model contains three critical footings with dimensions as follows: - (2.50 * 1.50) m, (2.0 * 1.0) and (1.0 * 1. 0) m respectively. Isolated footings have fixed depth (D) =0.5m connected with tie beams with variable width (b=0.6D, 0.7D, 0.8D, 0.9D and 1.0D) m and thickness (h=1.0D, 1.5D, 2.0D and 2.5D). A finite element package of the PLAXIS 3D-foundation version 15 has been used to simulate theoretically the model. All of the above assumptions have used with variable depth of footing (Df =0.0D, 0.5D, 1.0D and 1.5D). For eccentric loading it was found that the vertical displacement (settlement) and horizontal displacement under footings connected with tie beams decreases with increasing the thickness and width of tie beams by about (20 to 40)%. The settlement becomes almost uniform along axis and increasing the thickness and width of tie beam decrease the differential settlement. Also it was found that the values of the total normal stress (contact pressure) decrease with increasing width of tie beam and tie beam thickness by about (30 to 40)%. It was also found the bending moment as well as shear force values decrease with increasing the thickness and width of tie beams by about (30to 40 %).

Key words: Tie beam, Settlement, Contact pressure, Plaxis, Finite element, Eccentric, Footing

1.INTRODUCTION

In civil engineering constructions, foundations may be subjected to eccentric loads. Footing located at property lines and machine foundation are some examples where the foundations experience eccentric loading. If the load is eccentric-inclined, the stress distribution below the footing will be non-uniform causing unequal settlement at the two edges. Tie beams resting directly on soil are widely used to connect shallow footings, including strap or eccentric footing, in two directions. Practically, strap beam for eccentric footings are used with other tie beams. However, this system of beams and footings is considered as rigid and must be treated as one entity, where the tie beams play important role for redistribution of column loads between footings through it. El-Kasaby, E. A.A. (1993) [6] investigated the behavior of strap footings with tie-beam resting on soil. The effects of soil flexibility and beam stiffness on contact pressure, settlement and bending moment of strap foundation was presented. The finite difference technique was used and the elastic subgrade reaction theory was applied to study and solve the footing beam system. Partra, C. R., et all. (2005) [10] reported the results of model loading tests performed on an eccentrically loaded strip foundation supported by multi-layered geogrid-reinforced sand. Only one type of geogrid and sand at one relative density of compaction were considered. Based on the laboratory test results, an empirical relationship for the reduction factor was developed. This relationship can be used to estimate the ultimate bearing capacity under eccentric loading. Almasmoum A.A. (2009) [1] studied the influence of strap beams connected with eccentric footing and tie beams connected with centric interior footing on the contact pressure. The percentage of column loads transmitted by tie beams and the percentage ratio of vertical displacement to length of tie beam as well as maximum percentage ratio of differential displacement to length of tie beam were investigated. Sadoglu, E., et al. (2009) [13] investigated the decrease of the ultimate loads with increasing eccentricity and compare the experimental results with commonly used approaches. An experimental system was produced and used to run the tests. The experimental system consists of a tank, model footing, sand, loading mechanism, etc. A single woven geotextile sheet was placed horizontally below the footing's base at a depth of half of the footing's width. The measured decreases in ultimate loads with increasing eccentricities in the unreinforced tests within the core were in good agreement with Meyerhof's approach, while customary analysis is a little on the conservative side. Outside the core, Meyerhof's approach is on the conservative side in this case. Nawghare, S.M., et al. (2010) [9] investigated the bearing capacity of eccentrically loaded footing. Footings of different size and shape were used for testing. Testing for bearing capacity of centrally loaded footing and then for eccentrically loaded footing with different 'e/B' ratio was carried out. For every footing bearing capacity and settlement were found out for central as well as eccentric loading. These results of central and eccentric loading were compared with each other for same footing. The results of different footings were also compared for central and eccentric loading. By comparing these results effect of eccentricity, size and shape of footing on bearing capacity were investigated. Elsawaf, M. and Nazir, A. (2012) [8] presented an experimental study of the behavior of an eccentrically loaded model ring footing resting on a compacted replaced layer of soil that overlies on extended layer of loose sand. Load configuration was designed to simulate ring footing under vertical loads and overturning moment caused by lateral loads. The effect of the depth and relative density of the replaced sand layer were investigated. The results indicate that the behavior of an eccentrically loaded ring footing significantly improved with increasing the depth and the relative density of the replaced compacted sad layer.

Patra (2012) [12] conducted a number of laboratory model tests to determine the ultimate bearing capacity of strip foundation on sand subjected to vertical and inclined eccentric loads. Based on some of those laboratory test results, an empirical relationship has been developed to estimate the average settlement of the foundation while being subjected to an average allowable eccentric load per unit area, where the applied load is vertical. The empirical relationships presented were for embedment ratio Df/B varying from zero to one, and the eccentricity ratio e/B varying from zero to 0·15. Atalar, C., et al (2013) [2] determined the bearing capacity of shallow strip foundation subjected to eccentrically inclined load rested on dense sand. The embedment ratio (ratio of the depth of embedment Df to the width of the foundation B) was varied from zero to one. Load eccentricity (e) was varied from zero to 0.15B and the load inclination with the vertical (α) was varied from zero to 20 degrees. An empirical nondimensional reduction factor was developed. This reduction factor was the ratio of the bearing capacity of the foundation subjected to an eccentrically inclined load (average eccentrically inclined load per unit area) to the bearing capacity of the foundation subjected to a centric vertical load. Dhar, P., et al. (2013) [4] presented the results of laboratory model tests on behavior of a model footing resting on sand under eccentric – inclined load. Initially, the behavior of footing subjected to axial load was studied to compare with the shape factors at the surface footings. The influence of shape of footing on ultimate load carried capacity due to the different shape of model footings were investigated using bearing capacity ratio (BCR) a non-dimensional factor. The load settlement characteristics of footings of different shapes rested on the surface of sand of same area were also investigated through the load settlement curves. Pusadkar, S.S. Navkar, Y.S. (2016) [11] evaluated the effects of eccentricity and inclination of load along with eccentric-inclined load on performance of square footing resting over sand. A laboratory load tests were conducted on the model footing with eccentric load and/or inclined load. The results showed that the bearing capacity decreases with increasing the load eccentricity and load inclination. Dhatrak, A.I., et al. (2016) [5] presented the results of laboratory model tests on behavior of a model footing resting on sand under eccentric load. The ultimate load carrying capacity of a circular and ring footing resting on surface dense sand was investigated. The conventional method of footing design requires that footing must possess sufficient safety against failure and settlement was kept within the allowable value. Benayad, S., et al (2017) [3] examined the stresses distribution and contact pressure underneath eccentric footing subjected to the variation of its thickness and eccentricity using 2D finite element modeling. The FEM analysis was carried out using ABAQUS software program. The results indicated that stresses were higher along edges of footing than at center when footing is subjected to the variation of its thickness and eccentricity. The increase in footing thickness caused a decrease of maximum contact pressure and an increase in contact area. However, it could found that the maximum contact pressure increased proportionally with the increase in eccentricity, while contact surface decreased. Elsamny, M. K., et al (2017) [7] investigated the behavior of two isolated footings of different dimensions connected with tie beam. The dimensions of one footing were fixed. The width of the two footings was fixed (B=1.0m). The thicknesses of the two footings have variable (t=0.3B,0.4B,0.5Band0.6B). The tie beam between footings have variable lengths (Ltie=0.5B,1.0B,1.5B and 2.0B). The height of the tie beams was variable (h=1.0t,1.5t,2.0t and 2.5t) and the width of tie beam was fixed (b=0.25m). All of the above assumptions have used with variable effect of depth of footing (df=0.0B,0.5B,1.0B and 1.5B). In addition, the angle of internal friction in sandy soil was taken (Ø=30°,35°,40°and 45°). However, cohesion for clayey soil was taken as (c=10,15,20and 25) kN/m2. It was found that the vertical and horizontal displacement increased with increasing the length of tie beam. Also, the vertical and horizontal displacement decreased with increasing the angle of internal friction in sandy soil as well as cohesion in clayey soil. The vertical and horizontal displacement decreased with increasing the height of tie beam.

2. FINITE ELEMENT PROGRAM

A finite element package of the PLAXIS 3D-foundation version 15 has been used for in order to simulate the chosen model. Mohr-Coulomb model has been used to represent the soil behavior. The material properties for soil, tie beams and foundations which have been used in the finite element model are shown in table (1) and table (2).

Table 1 The material properties for the used soil

Parameters	sandy soil	unit
Unsaturated soil weight	17	(kN/m^3)
Saturated soil weight	20	(kN/m^3)
Modules of elasticity of soil	20000 - 70000	(kN/m^2)
Poisson ratio	0.30	
Thickness of footing	0.50	(m)
Angle of internal friction	30˚, 35˚, 40˚ and 45˚	˚
Dilatancy	0,5,10 and 15	˚

Table 2 Investigated cases of study

Case No.	**Tie Beam Dimensions [m]**	
	Breadth	**Thickness**
1		1.00 D
2		1.25 D
3	0.6D	1.50 D
4		1.75 D
5		2.00 D
6		1.00 D
7		1.25 D
8	0.7D	1.50 D
9		1.75 D
10		2.00 D
11		1.00 D
12		1.25 D
13	0.8D	1.50 D
14		1.75 D
15		2.00 D
16		1.00 D
17		1.25 D
18	0.9D	1.50 D
19		1.75 D
20		2.00 D
21		1.00 D
22		1.25 D
23	1D	1.50 D
24		1.75 D
25		2.00 D

In the present study, a theoretical analysis has been done for model of neighbors from two sides contains 16 footings connected with tie beam. Figures (1) and (2) presented the chosen model. The footing dimensions are (2.0*2.0) m for corner footings, (2.50*2.50) m for edge footings and (3.0*3.0) m for middle footings. The model contains three critical footings (F1, F2 and F3) with dimensions (2.50 * 1.50) m, (2.0 * 1.0) and (1.0 * 1. 0) m respectively. Isolated footings have fixed depth =0.5m connected with tie beams with variable width (b=0.6D, 0.7D, 0.8D, 0.9D and 1.0D) and variable thickness (h=1.0D, 1.5D, 2.0D and 2.5D). The angle of internal friction in sandy soil has been taken (Ø=30°, 35°, 40°and 45°). All of the above assumptions have done with variable effect of depth of footing (Df =0.0D, 0.5D, 1.0D and 1.5D).

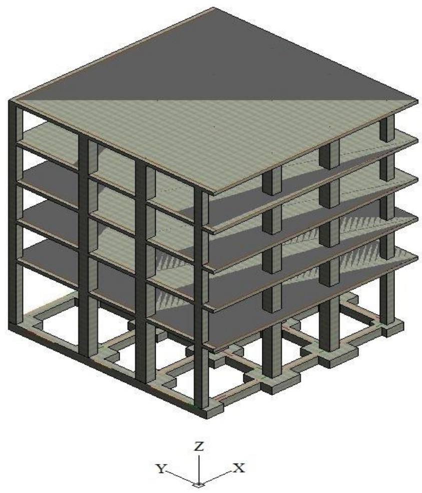

Figure 1 Model of neighbours from two sides

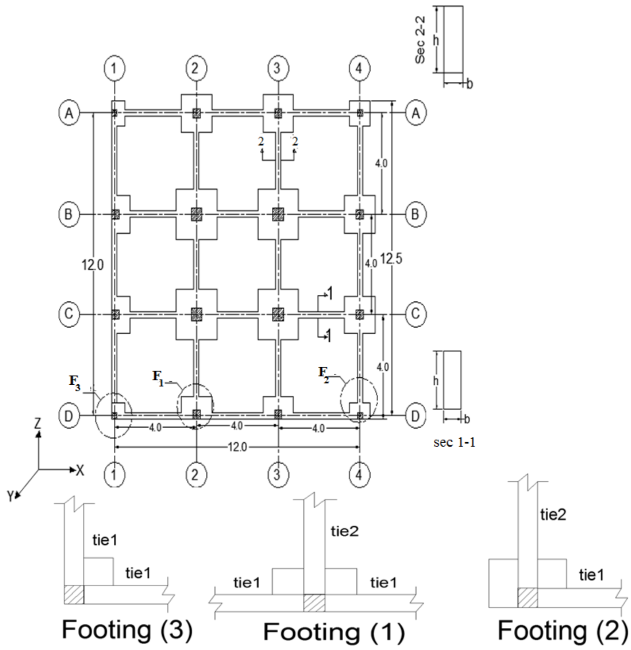

Figure 2 Isolated footings connected with beams model

3. RESULTS OF FINITE ELEMENT

Figures from (3) to (5) show the deformed mesh of soil and vertical displacement of soil as contour lines as well as shading at depth of footing=0.50D, thickness of tie (ht)=1.0D, width of tie(bt)=0.6D and angle of internal friction(φ)=30^{0}. From these figures, it can be shown that the footings act as one combined footing.

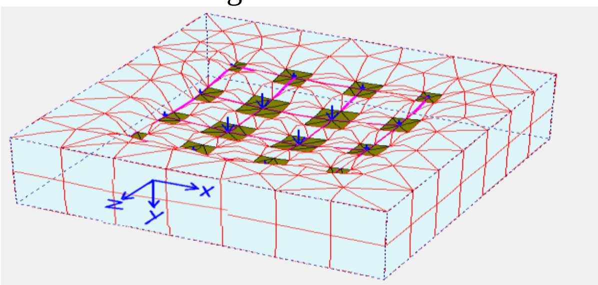

Figure 3 Deformed mesh of soil at depth of footing (0.50)D and angle of internal friction (φ) = 30˚ for sand soil b_t =0.6D and h_t =1.00D)

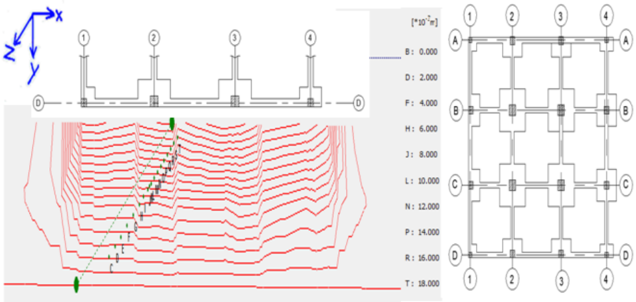

Figure 4 Total displacements in soil as contour lines for angle of internal friction (φ) = 30˚, bt =0.6D, Df = (0.50)D and ht =1.00D) at axis (D)

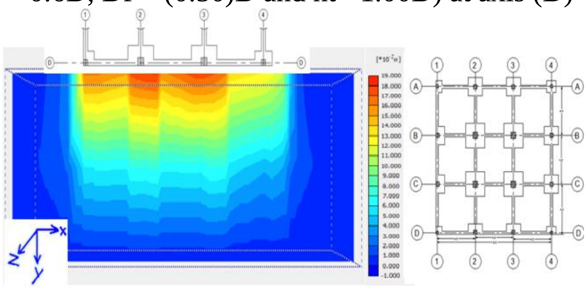

Figure 5 Total displacements in soil as shading for angle of internal friction (φ) = 30˚, b_t =0.6D, Df = (0.50)D and h_t =1.00D) at axis (D)

Figures from (6) to (8) show the deformed mesh of soil and vertical displacement of soil as contour lines as well as shading at depth of footing=0.50D, thickness of tie (ht)=1.50D, width of tie(bt)=0.6D and angle of internal friction(φ)=30^{0}. From these figures, it can be shown that the footings act as one combined footing.

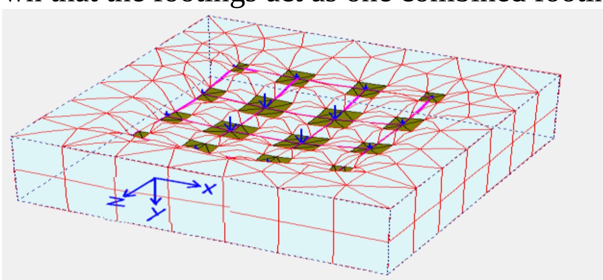

Figure 6 Deformed mesh of soil at depth of footing (0.50D) and angle of internal friction (φ) = 30˚ for sand soil b_t =0.6D and h_t =1.50D)

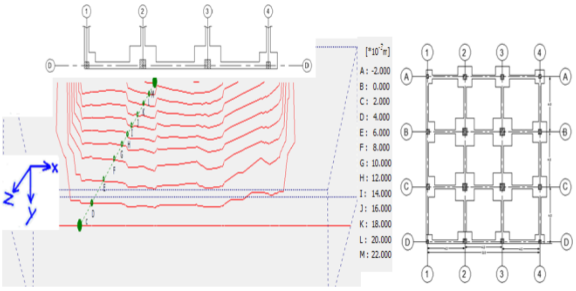

Figure 7 Total displacements in soil as contour lines for angle of internal friction (φ) = 30˚, b_t =0.6D, Df = (0.50)D and h_t =1.50D) at axis (D)

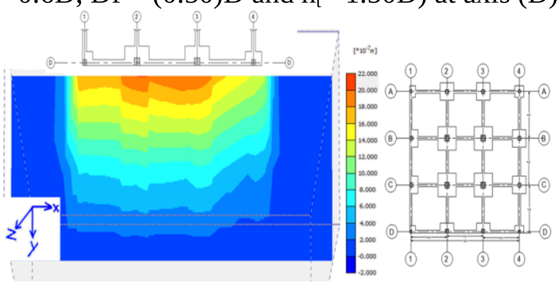

Figure 8 Total displacements in soil as shading for angle of internal friction (φ) = 30˚, b_t =0.6D, Df = (0.50)D and h_t =1.50D) at axis (D)

Figures from (9) to (11) show the deformed mesh of soil and vertical displacement of soil as contour lines as well as shading at depth of footing=1.50D, thickness of tie (ht)=1.0D, width of tie(bt)=1.0D and angle of internal friction(φ)=30^0. From these figures, it can be shown that the footings act as one combined footing.

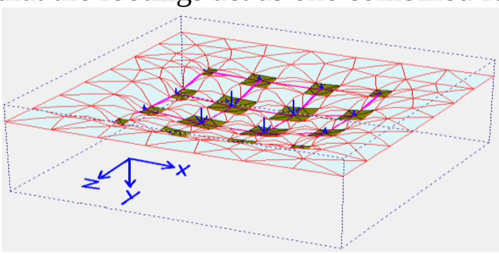

Figure 9 Deformed mesh of soil at depth of footing (1.50)D and angle of internal friction (φ) = 30˚ for sand soil b_t =1.0D and h_t =1.00D)

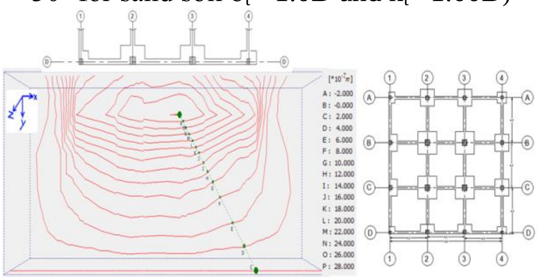

Figure 10 Total displacements in soil as contour lines for at depth of footing (1.50)D and angle of internal friction (φ) = 30˚ for sand soil b_t =1.0D and h_t =1.00D)

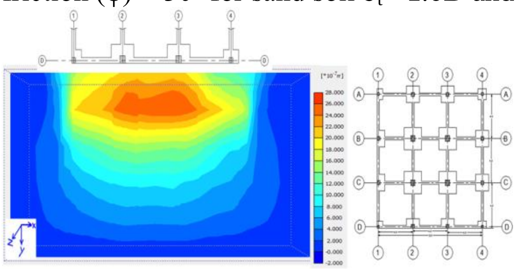

Figure 11 Total displacements in soil as shading at depth of footing (1.50)D and angle of internal friction (φ) = 30˚ for sand soil b_t =1.0D and h_t =1.00D)

Figures (12) and (13) show the settlement under footing (F2) at different tie beam dimensions at depth of footing D_f=0.0D along x-axis. From these figures, it can be shown that the settlement decreases with increasing the dimensions of tie beams by about (20 to 40)%.

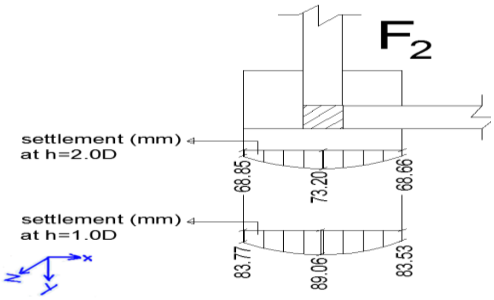

Figure 12 Distribution of settlement under footing for different thickness of tie beam at (b_{T1} =0.6D) and D_f=0.0D along x-axis

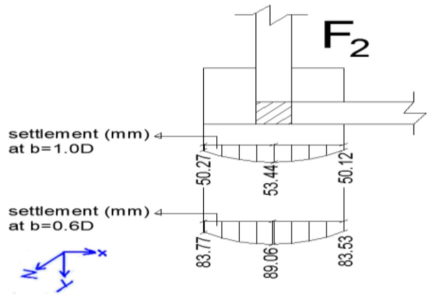

Figure 13 Distribution of settlement under footing for different thickness of tie beam at (h_{T1} =1.0D) and D_f=0.0D along x-axis

Figures (14) and (15) show the settlement under footing (F2) at different tie beam dimensions at depth of footing D_f=0.0D along z-axis. From these figures, it can be shown that the settlement decreases with increasing the dimensions of tie beams by about (20 to40)%.

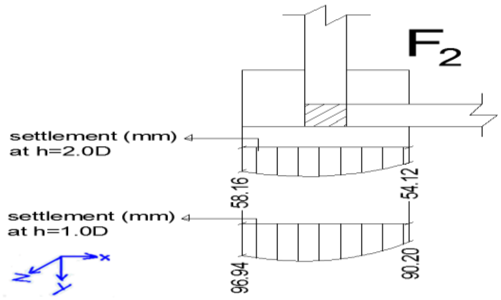

Figure 14 Distribution of settlement under footing for different thickness of tie beam at (b_{T1} =0.6D) and D_f=0.0D along z-axis

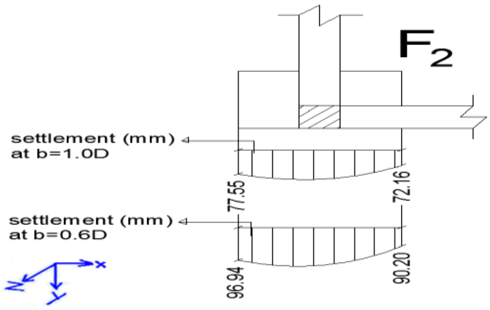

Figure 15 Distribution of settlement under footing for different thickness of tie beam at (h_{T1} =1.0D) and D_f=0.0D along z-axis

Figures (16) and (17) show the contact pressure under footing (F2) at different tie beam dimensions at depth of footing D_f=0.0D along x-axis. From these figures, it can be shown that the contact pressure values decrease with increasing the dimensions of tie beams by about (30 to 40)%.

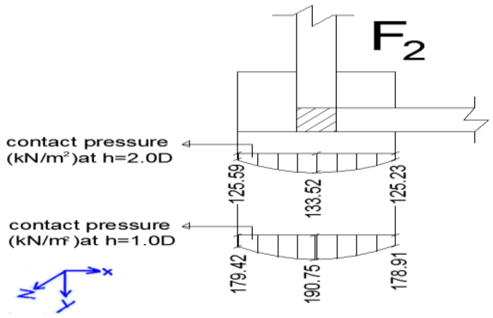

Figure 16 Distribution of contact pressure under footing for different thickness of tie beam at (b_{T1} =0.6D) and D_f=0.0D along x-axis

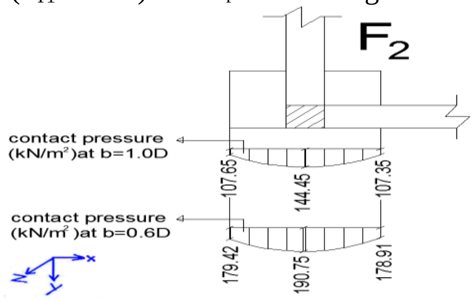

Figure 17 Distribution of contact pressure under footing for different thickness of tie beam at (h_{T1} =1.0D) and D_f=0.0D along x-axis

Figures (18) and (19) show the contact pressure under footing (F2) at different tie beam dimensions at depth of footing Df=0.0D along z-axis. From these figures, it can be shown that the settlement decreases with increasing the dimensions of tie beams by about (30 to40)%.

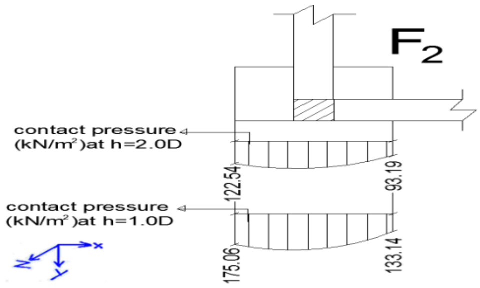

Figure 18 Distribution of contact pressure under footing for different thickness of tie beam at (b_{T1} =0.6D) and D_f=0.0D along z-axis

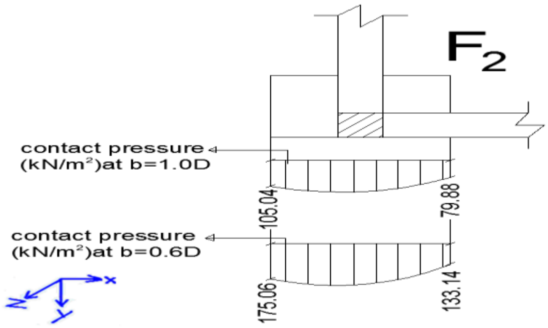

Figure 19 Distribution of contact pressure under footing for different thickness of tie beam at (h_{T1} =1.0D) and D_f=0.0D along z-axis

Figures (20) and (21) show the settlement under footing (F3) at different tie beam dimensions at depth of footing D_f=0.0D. From these figures, it can be shown that the settlement decreases with increasing the dimensions of tie beams by about (20 to40)%.

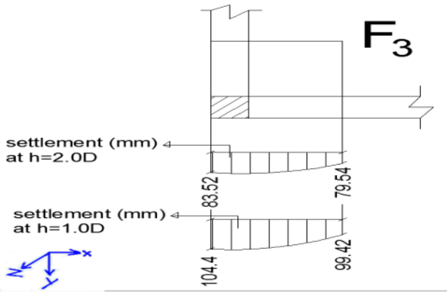

Figure 20 Distribution of settlement under footing for different thickness of tie beam at (b_{T1} =0.6D) and D_f=0.0D

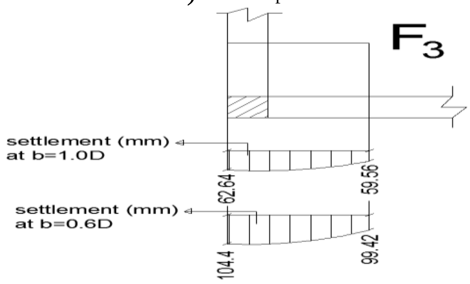

Figure 21 Distribution of settlement under footing for different thickness of tie beam at (h_{T1} =1.0D) and D_f=0.0D

Figures (22) and (23) show the contact pressure under footing (F2) at different tie beam dimensions at depth of footing D_f=0.0D.

From these figures, it can be shown that the contact pressure values decrease with increasing the dimensions of tie beams by about (30 to40)%.

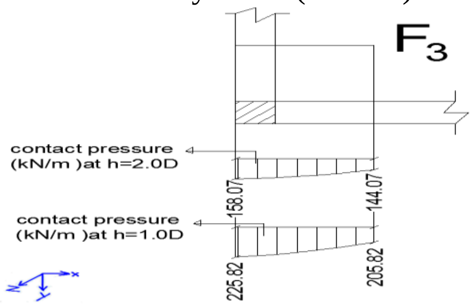

Figure 22 Distribution of contact pressure under footing for different thickness of tie beam at (b_{T1} =0.6D) and D_f=0.0D

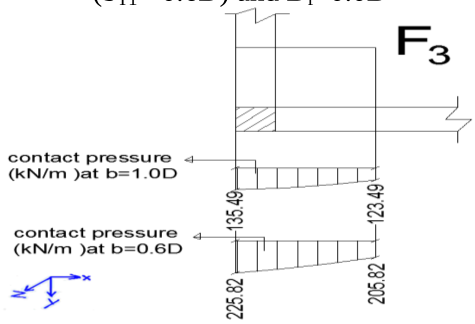

Figure 23 Distribution of contact pressure under footing for different thickness of tie beam at (h_{T1} =1.0D) and D_f=0.0D

4. ANALYSIS OF RESULTS

Figures (24) and (25) show the effect of tie beam dimensions on settlement for footing (1). These figures show that the settlement decreases with increasing tie beam thickness and width. However, increasing tie beam dimensions decreases the settlement by about (20-40)%.

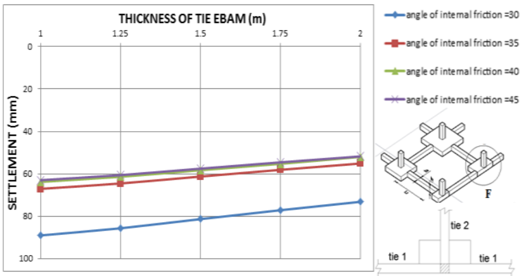

Figure 24 Comparison between thickness of tie beam and settlement for different angles of internal friction (φ) at D_F= 0.00D and b_{T1} = 0.6D

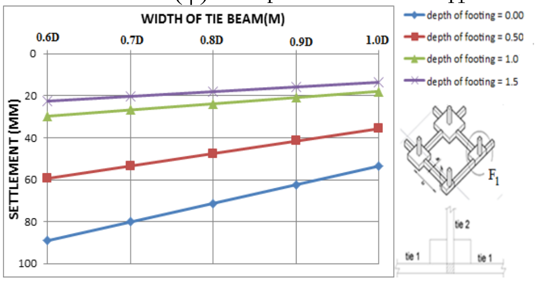

Figure 25 Comparison between width of tie beam and settlement for different depths of footing at angle of internal friction Φ = 30° and h_{T1} = 1.0D

Figures (26) and (27) show the effect of tie beam dimensions on contact pressure values for footing (1). From these figures the contact pressure values decrease with increasing the thickness and width of tie beam. However, increasing the dimensions of tie beam decrease the contact pressure values by about (30-40)%.

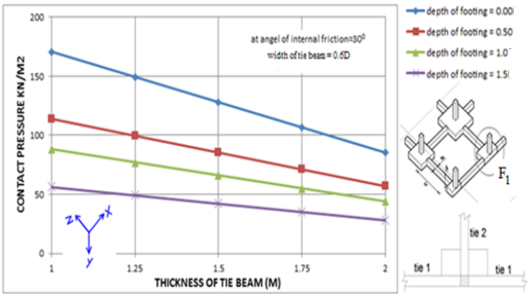

Figure 26 Relationship between contact pressure and thickness of tie beam for different depths of footing at angle of internal friction Φ = 30° and b_{T1} = 0.6D

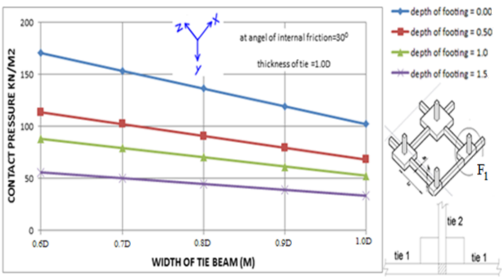

Figure 27 Relationship between contact pressure and width of tie beam for different depths of footing at angle of internal friction Φ = 30° and h_{T1} = 1.0D

Figures (28) and (29) show the effect of tie beam dimensions and depth of footing on settlement for footing (2). These figures show that increasing the thickness of tie beam from 1.0D to 2.0D decreases the settlement by about 20% as well as increasing tie beam width from 0.6D to 1.0D decreases the settlement by about 40%.

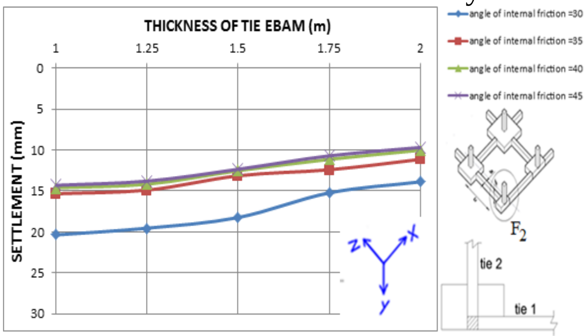

Figure 28 Comparison between thickness of tie beam and settlement for different angles of internal friction (φ) at D_F= 0.00D and b_{T2} = 0.6D

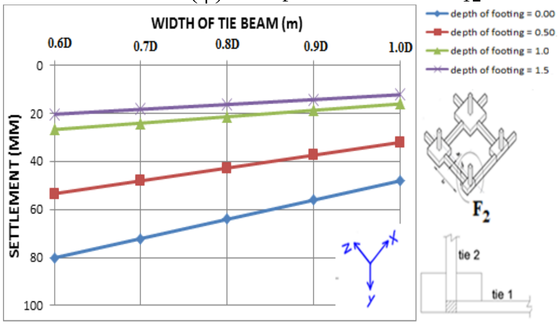

Figure 29 Comparison between width of tie beam and settlement for different depths of footing at angle of internal friction (φ) = 30^0 and h_{T2} = 1.0D

Figures (30) and (31) show the effect of tie beam dimensions at different depths of footing on contact pressure values for footing (2). From these figures the contact pressure values decrease with increasing the thickness and width of tie beam.

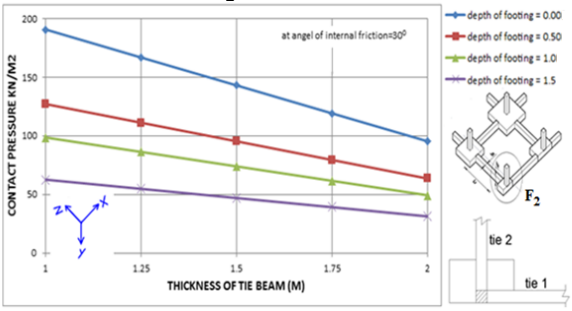

Figure 30 Relationship between contact pressure and thickness of tie beam for different depths of footing at angle of internal friction Φ = 30° and b_{T1} = 0.6D

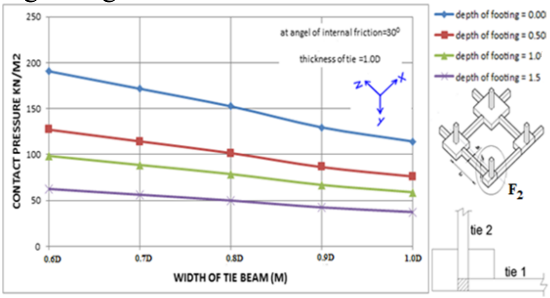

Figure 31 Relationship between contact pressure and width of tie beam for different depths of footing at angle of internal friction Φ = 30° and h_{T1} = 1.0D

Figures (32) and (33) show the effect of tie beam dimensions and depth of footing on settlement for footing (3). These figures show that the settlement decreases by 20% with increasing thickness from 1.0D to 2.0D as well as increasing the width of tie beam from 0.6D to 1.0D decreases the settlement by about 40%.

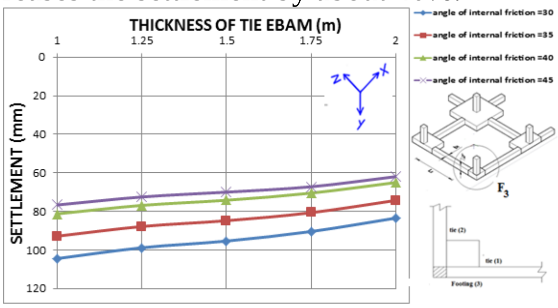

Figure 32 Comparison between tie beam thickness and settlement for angles of internal friction (φ) at D_f= 0.00D and b_{T1} = 0.6D

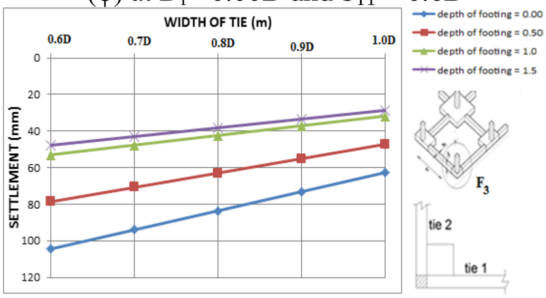

Figure 33 Comparison between width of tie beam and settlement for different depths of footing at D_f= 0.00D and h_{T1} = 1.0D

Figures (34) and (35) show the effect of tie beam dimensions for different depths of footing on contact pressure values for footing (3). From these figures the contact pressure values decrease with increasing tie beam thickness and width by about (30-40)%.

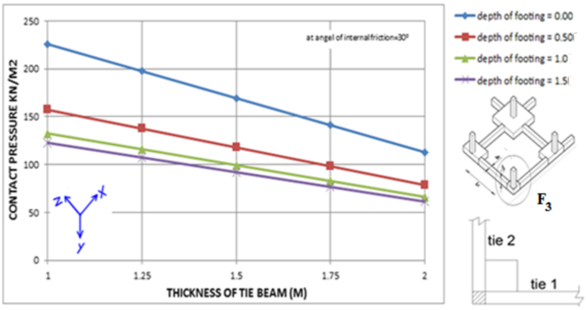

Figure 34 Relationship between contact pressure and thickness of tie beam for different depths of footing at angle of internal friction $\Phi = 30°$ and $b_{T1} = b_{T2} = 0.6D$

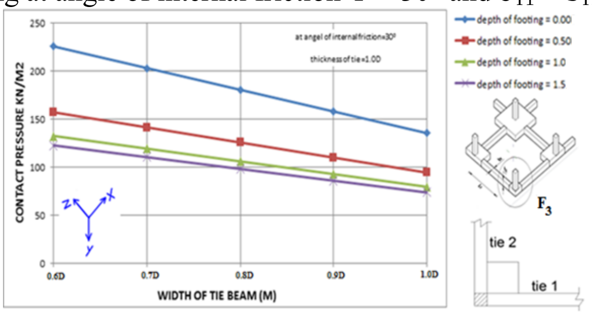

Figure 35 Relationship between contact pressure and width of tie beam for different depths of footing at angle of internal friction $\Phi = 30°$ and $h_{T1} = h_{T2} = 1.0D$

Figures (36) and (37) show the effect of tie beam dimensions and depth of footing on horizontal displacement in x and z direction. From these figures the horizontal displacement in x and z directions decreases with increasing the thickness and width of tie beam. However, increasing the tie beam dimensions decreases the displacement by about (20-40)%.

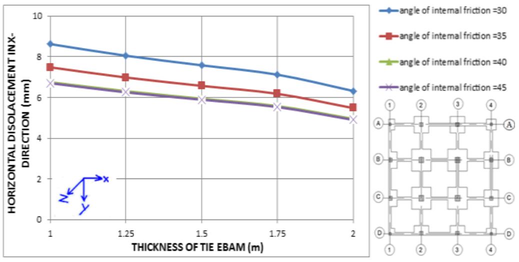

Figure 36 Comparison between thickness of tie beam and displacement in x- direction for different angles of internal friction (φ) at D_F = 0.00D and b_{T1} = 0.6D

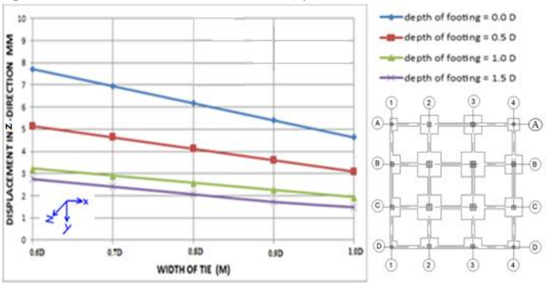

Figure 37 Comparison between width of tie beam and displacement in z- direction for different depths of footing at D_f= 0.00D and h_{T1} = 1.0D

Figures (38) to (40) show the relationship between settlement and distance along axis's (D , 2 and 4) for different thickness of tie beam at width of tie beam (b_{T1}) =0.6D, depth of footing D_f = 0.0D and angle of internal friction=30^0. From these figures increasing the thickness and width of tie beam decrease the settlement. However increasing thickness and width of tie beam decrease the differential settlement and almost uniform settlement has been obtained.

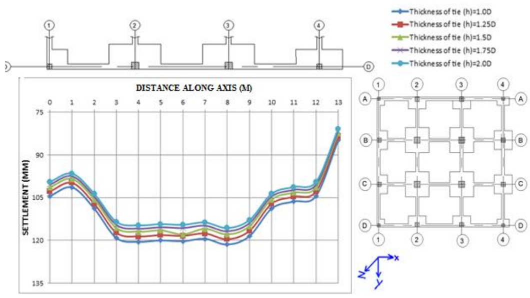

Figure 38 Relationship between settlement and distance along axis (D) for different thickness of tie beam at angle of internal friction = 30^0, b_{T1}= b_{T2}=0.6D and D_F=0.0D

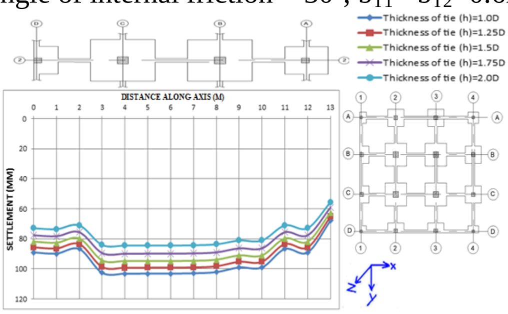

Figure 39 Relationship between settlement and distance along axis (2) for different thickness of tie beam at angle of internal friction = 30^0, b_{T1} =0.6D and D_F=0.0D

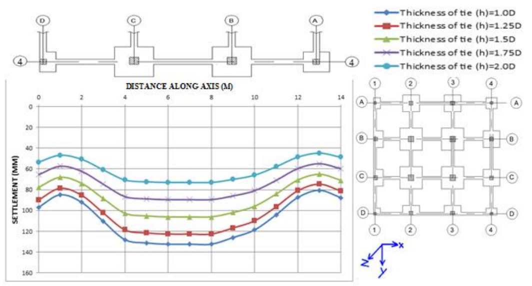

Figure 40 Relationship between settlement and distance along axis (4) for different thickness of tie beam at angle of internal friction = 30^0, b_{T1} =0.6D and D_F=0.0D

Figure (41) shows the relationship between settlement and distance along axis (D) for different widths of tie beam at thickness of tie beam (h_{T1}) = (h_{T2}) =1.0D, depth of footing D_f = 0.0D and angle of internal friction=30^0. From this figure increasing the width of tie beam from 0.6D to 1.0D decreases the settlement by about 40%.

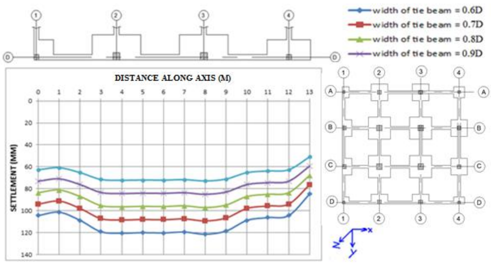

Figure 41 relationship between settlement and distance along axis (D) for different widths of tie beam at angle of internal friction = 30^0, D_F= (0.0) D and h_{T1}= h_{T2}=1.0D

Figures (42) to (44) show the relationship between contact pressure and distance along axis's (D, 2 and 4) for different thickness of tie beam at width of tie beam (b_{T1}) =0.6D, depth of footing D_f = 0.0D and angle of internal friction=30^0. From these figures increasing the thickness of tie beam from 1.0D to 2.0D decreases the contact pressure values by about 30%.

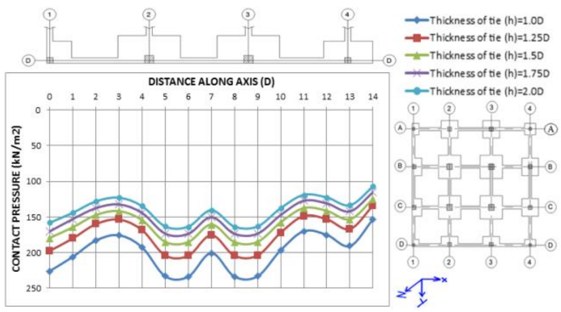

Figure 42 Relationship between contact pressure and distance along axis (D) for different thickness of tie beam at angle of internal friction = 30^0, b_{T1} = b_{T2} = 0.6D and D_F=0.0D

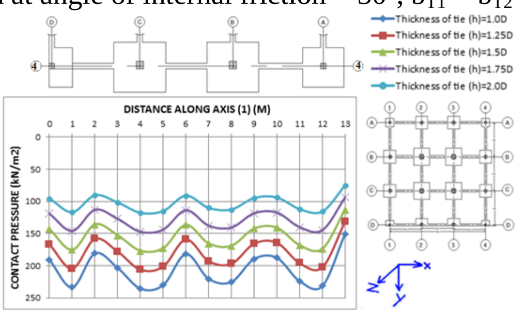

Figure 43 Relationship between contact pressure and distance axis (4) for different thickness of tie beam at angle of internal friction = 30^0, b_{T1}=0.6D and D_F=0.0D

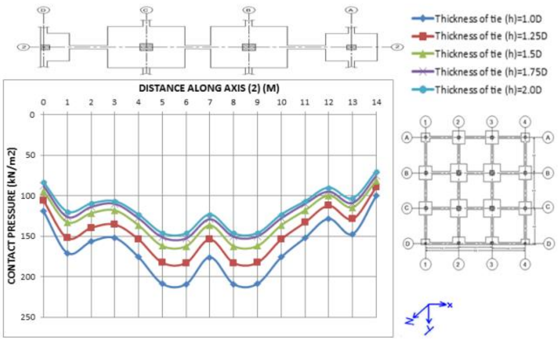

Figure 44 Relationship between contact pressure and distance along axis (2) for different thickness of tie beam at angle of internal friction = 30^0, b_{T1}=0.6D and D_F=0.0D

Figures (45) to (47) show the relationship between contact pressure and distance along axis's (D,2 and 4) for different widths of tie beam at thickness of tie beam (h_{T1}) = (h_{T2}) =1.0D, depth of footing D_f = 0.0D and angle of internal friction=30^0. From this figure increasing the thickness of tie beam from 0.6D to 1.0D decreases the contact pressure values by about 40%.

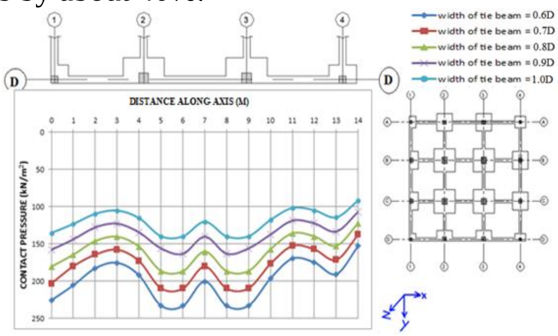

Figure 45 Relationship between contact pressure and distance along axis (D) for different widths of tie beam at angle of internal friction = 30^0, D_F = 0.0D and h_{T1} = h_{T2} = 1.0D

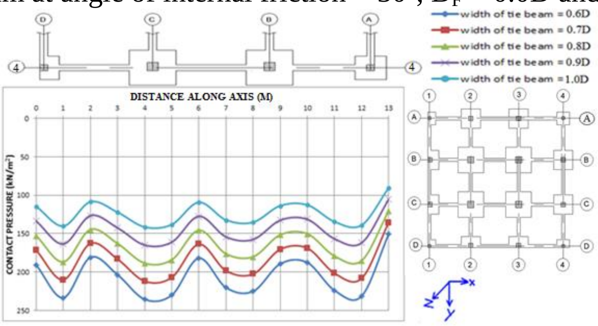

Figure 46 Relationship between contact pressure and distance along axis (4) for different widths of tie beam at angle of internal friction = 30^0, h_{T2}=1.0D and D_F=0.0D

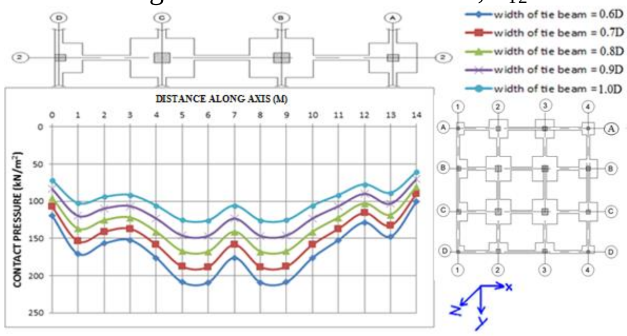

Figure 47 Relationship between contact pressure and distance along axis (2) for different widths of tie beam at angle of internal friction = 30^0, D_F = 0.0D and h_{T1}=1.0D

Figures (48) to (51) show the distribution of bending moment of beam- footing system along axis's (D, 2 and 4) and dimensions of tie beam at angle of internal friction = 30^0. From this figure the bending moment values decrease with increasing the dimensions (thickness and width) of tie beam. However, increasing the dimensions of tie beam decrease the bending moment values by about (30 to 40)%.

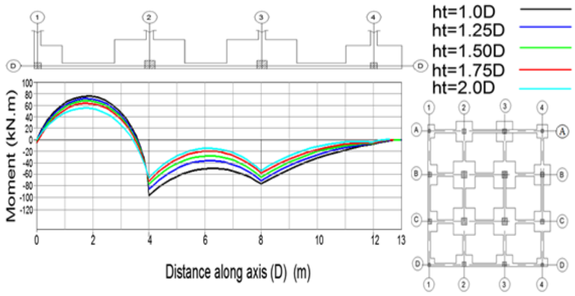

Figure 48 Distribution of bending moment of beam- footing system along axis (D) for different thickness of tie beam at angle of internal friction = 30^0 and b_{T1} = 0.6D

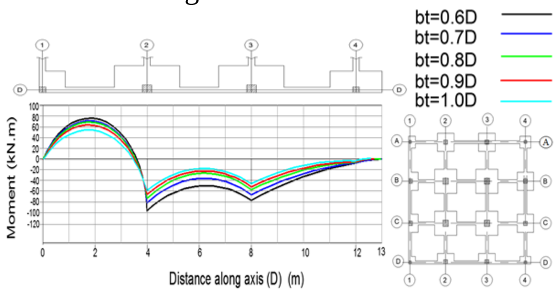

Figure 49 Distribution of bending moment of beam- footing system along axis (D) for different widths of tie beam at angle of internal friction = 30^0 and h_{T1} = 1.0D

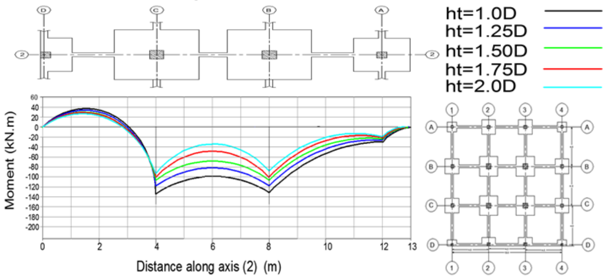

Figure 50 Distribution of bending moment of beam- footing system along axis (2) for different thickness of tie beam at angle of internal friction = 30^0 and b_{T2} = 0.6D

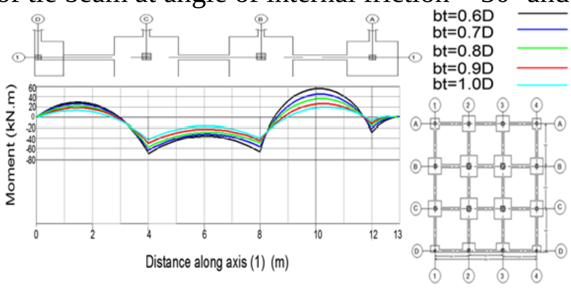

Figure 51 Distribution of bending moment of beam- footing system along axis (4) for different widths of tie beam at angle of internal friction = 30^0 and h_{T2} = 1.0D

Figures (52) to (54) show the distribution of shear force diagram of beam- footing system along axis's (D and 2) and dimensions of tie beam at angle of internal friction = 30^0. From these figures the shear force values decrease with increasing the dimensions (thickness and width) of tie beam. However, increasing the dimensions of tie beam decrease the bending moment values by about (30 to 40)%.

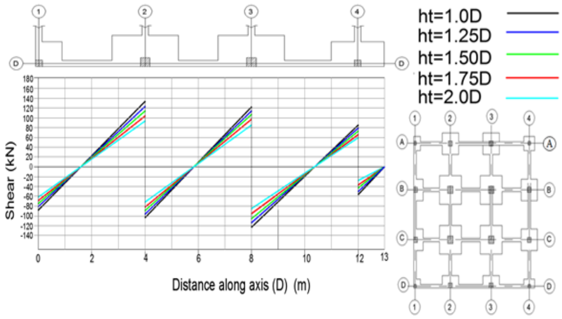

Figure 52 Distribution of shear of beam- footing system along axis (D) for different thickness of tie beam at angle of internal friction = 30^0 and b_{T1} = 0.6D

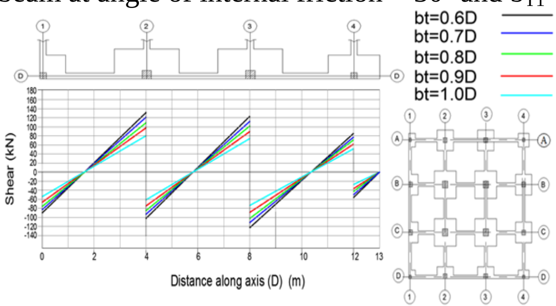

Figure 53 Distribution of shear of beam- footing system along axis (D) for different tie beam widths at angle of internal friction = 30^0 and h_{T1} = 1.0D

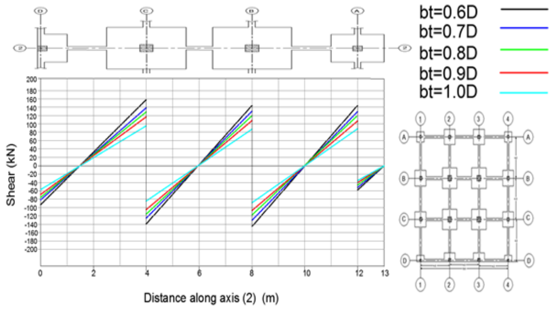

Figure 54 Distribution of shear of beam- footing system along axis (2) for different tie beam widths at angle of internal friction = 30^0 and h_{T1} = 1.0D

5. CONCLUSIONS

From the present study the followings are concluded:-

- The settlement under footings and horizontal displacement in both x and z directions decrease with increasing thickness and width of tie beams by about (20 to 40)%.
- Increasing the thickness and width of tie beam decrease the settlement. However, increasing the thickness and width of tie beam decrease the differntial settlement and almost uniform has been obtained.
- The contact pressure values decrease with increasing the thickness and width of tie beam by about 30 to 40%.
- The bending moment values decrease with increasing the thickness and width of tie beams by about 30 to 40%.
- The shear force values decrease with increasing the thickness and width of tie beams by about 30 to 40%.

6. REFERENCES

[1] Almasmoum A.A. (2009) "influence of tie beams on the shallow isolated eccentric footing system" Journal of Engineering Sciences, Assiut University, Vol. 37, No. 1, pp.51 -61, January 2009

[2] Atalar, C., C. R. Patra, C.R. and Sivakugan, N (2013) "Bearing capacity of shallow foundation under eccentrically inclined load" Conference: 18th International Conference on Soil Mechanics and Geotechnical Engineering, At Paris, France, Volume: 4

[3] Benayad,S., Berga, A. and Sadek, Y. (2017) " Influence of eccentric footing thickness on contact pressure and stress distribution at interface" International Journal of Civil Engineering and Technology (IJCIET)- http://www.iaeme.com/IJCIET/index.asp

[4] Dhar, P., Roy, S.and chattapadhyay, B. C. (2013) "Behavior of Rigid Footing under Inclined and Eccentric Loading" Annals of Pure and Applied Mathematics, Vol. 5, No.1, 2013, 71-81, ISSN: 2279-087X (P), 2279-0888(online), www.researchmathsci.org

[5] Dhatrak, A.I. and Poonam Gawande (2016) "Behaviour of Circular and Ring Footing on Reinforced Sand" ISSN XXXX XXXX © 2016 IJESC, Volume 6 Issue No. 8

[6] El-Kasaby, E. A. A. (1993), "Behavior Of Strap Footings With Tie-Beam Resting On Soil", Civil Engineering Research Magazine, Faculty Of Engineering Al-Azhar University Cairo Egypt, Vol. 15, No. 6, PP. 47-59.

[7] Elsamny, M. K., Ezz-Eldeen, H.A.,ELbatal. S.A. and kamar, A. M.(2017), “Effect of tie beam dimensions on vertical and horizontal displacement of isolated footing” , International Journal of Engineering Research&Technology, Faculty of, Vol. 6 Issue 04, April-2017.

[8] Elsawaf, M. and Nazir, A. (2012)"Behavior of eccentrically loaded small-Scale ring footing resting on reinforced layered soil" DOI: 10.1061/(ASCE)GT.19435606.0000593.@2012 American Society of Civil Engineers.

[9] Nawghare, S.M., Pathak, S.R. and Gawande, S.H. (2010) "Experimental investigations of bearing capacity for eccentrically loaded footing" S. M. Nawghare et al. / International Journal of Engineering Science and Technology, Vol. 2(10), 2010, 5257-5264

[10] Partra, C. R., Das, B.M. and Shin, E.C. (2005)" Ultimate bearing capacity of eccentrically loaded strip foundation on sand reinforced with geogrids" Archived with Dspace@nitr, http://dspace.nitrkl.ac.in/dspace, 8to 9 December 2005, Bangkok.

[11] Pusadkar, S.S. and Navkar, Y.S. (2016) "Performance of Square Footing Subjected to Eccentric-Inclined Load" International Journal of Engineering Research Volume No.5, Issue Special 1 pp : 44-46, ISSN:2319-6890(online),2347-5013(print) 8 & 9 Jan 2016

[12] Partra, C. R. (2012)" Behaviour of eccentrically loaded shallow foundations on granular soil" A thesis submitted in partial fulfillment of the requirements for the degree of Master of Technology in Civil Engineering, department of civil engineering national institute of technology rourkela-769008, may 2013

[13] Sadoglu, E., Cure, E., Moroglu, B. and Ulzuner, B.A. (2009)" Ultimate loads for eccentrically loaded model shallow strip footings ongeotextile-reinforced sand" Geotextiles and Geomembranes 27 (2009) 176–182, journal homepage:www.elsevier.com/locate/geotexm